Generation of Monodisperse, Shape-Controlled Single and Hybrid Core–Shell Nanoparticles via a Simple One-Step Process

*Jong-Seon Kim, Hwan-Jin Jeon, Hae-Wook Yoo, Youn-Kyoung Baek, Kyoung Hwan Kim, Dae Woo Kim, and Hee-Tae Jung**

In nano-biotechnology, optoelectronics, and energy research areas, various fabrication methods have been developed for hybrid nanoparticles. A method is developed here for fabricating highly monodisperse three-dimensional hybrid nanoparticles using a unique top-down method based on secondary sputtering lithography. Nanostructures that have been formed on a PEDOT sacrificial layer are transferred from the substrate to an aqueous solution in a process that could be used to successfully disperse a variety of nanoparticle shapes and hybrid nanoparticles. By this method, a fluorescent dye could be encapsulated within the fabricated hybrid nanoparticles for use in bio-sensing and drug-delivery applications

1. Introduction

The fabrication and manipulation of monodisperse, 3D nanoparticles with inorganic/inorganic or inorganic/organic hybrid core–shell structures is an important issue in nanobiotechnology,[1–5] optoelectronics,[6,7] magnetic application[8] and energy[9,10] research. The optical and electrical properties of each component may be selected under particular design constraints to obtain a variety of materials for specific end-use applications. As in the fabrication of single-component nanoparticles, hybrid nanoparticles must be fabricated in such a way as to obtain highly monodisperse and uniform 3D shapes with features on the micrometer and subnanometer scales.[8,11–13] Such fabrication specifications are necessary for many applications. The introduction of inorganic and organic chemical functionalities onto a nanoparticle surface is difficult, not to mention achieving control over the size and shape of the hybrid nanoparticles. Most conventional fabrication methods depend on chemical reactions or the shapes of seed particles, neither of which principle is sufficiently flexible for application to hybrid nanoparticle fabrication.[14] Currently, Wang's group developed the top-down fabrication method using tri-layered nanostructure and methal deposition,[8] but the method has a limitation for size and shape control.

As lithography technologies develop, many inexpensive top-down lithography approaches enable to fabricate over 10nm.[15–18] Several approaches have been suggested for fabricating hybrid nanoparticles with shape and size control, including particle replication in nonwetting templates (PRINT)[19–23] vapor deposition polymerization (VDP),[24,25] surface polymerization methods,[26,27] and chemical reduction methods.[28–30] PRINT method is very powerful method to obtain various shaped and biomaterial particle by using low-surface energy and chemically resistant fluoropolymers as molding materials.[19] DeSimone group developed the method in 2005[19] and they have improved for various composition particle fabrication as a protein particle,[20] CdSe quantum dot,[21] hydrogel particle.[22] Recently, they developed a multiphase rod-like particle fabrication method modified PRINT method for tunable self-assembly application.[23] But, inorganic/organic hybrid nanoparticle fabrication is not acheived from the method. VDP processes introduce surface modifications onto SiO_2 or TiO_2 colloidal particles via a vinyl polymer layer that forms inorganic colloidal core/vinyl polymer shell nanoparticles. The thickness of the vinyl polymer layer could be varied by controlling the polymerization process time. Surface polymerization methods have been used primarily to fabricate polymer–magnetite hybrid nanoparticles consisting of Fe_3O_4 cores and organic shells because Fe_3O_4 has a strong affinity toward polymers that are amenable to RAFT polymerization or ring-opening polymerization reactions. Recently, Xue et al. fabricated Au/Ag core–shell nanoprisms using chemical reduction methods.[28] A Ag nanoparticle solution was irradiated with a halogen lamp to induce anisotropic nanoparticle growth in a prism shape. Gold precursor ions ($AuCl_4^-$ and $AuCl_2^-$) were then added to form a thin Au coating layer on the Ag prisms. The Au precursors were found to etch the Ag nanoprisms in a galvanic replacement reaction.[31] To minimize the etching

J.-S. Kim, H.-J. Jeon, H.-W. Yoo, K. H. Kim, D. W. Kim, Prof. H.-T. Jung
Department of Chemical and Biomolecular Engineering
Korea Advanced Institute of Science and Technology (KAIST)
335 Gwahangno, Yuseong-gu, Daejeon, 305–701, Korea
E-mail: heetae@kaist.ac.kr
Dr. Y.-K. Baek
Powder & Ceramic Division
Korea Institute of Materials Science (KIMS)
797 Changwondaero, Seongsan-gu, Changwon, 642–831, Korea

DOI: 10.1002/adfm.201302494

reaction, hydroxylamine (HyA) was added to the solution to promote the epitaxial growth of Au on the prepared Ag nanoprisms. Other conventional chemical methods have faced similar difficulties. In the context of methods that rely on chemical reactions, the composition of a hybrid nanoparticle will always depend on the affinity between the core material and the shell material. Despite many efforts to control nanoparticle shape using chemical approaches, the fabrication of complex core–shell hybrid structures with a narrow size distribution has remained a challenge.

Here, we report a new and highly reliable approach to the fabrication of 3D complex single and hybrid nanoparticles with a monodisperse size distribution. A secondary sputtering lithography (SSL) approach[32–34] was used to fabricate the nanostructures, in which target inorganic materials on a substrate were etched and then deposited onto the surface of a pre-patterned organic or inorganic structure. Etching of the patterned structures yielded single nanoparticles, whereas the absence of the etching step yielded hybrid nanoparticles. A water-soluble PEDOT sacrificial layer under the target inorganic material facilitated the release of the complex 3D nanoparticles by dissolution of the PEDOT layer in an aqueous solution. The nanostructures fabricated by this approach were highly monodisperse and displayed a variety of single or hybrid nanoparticle shapes, including cylinders, glasses, chairs, and bowls. The size and shape of a particle could be controlled by changing the etching time and angle. This method may be applied toward the fabrication of many monodisperse organic, inorganic, or hybrid nanostructures with complex shapes. Bi-functional hybrid nanoparticles may potentially be useful as drug delivery carriers or sensing materials.

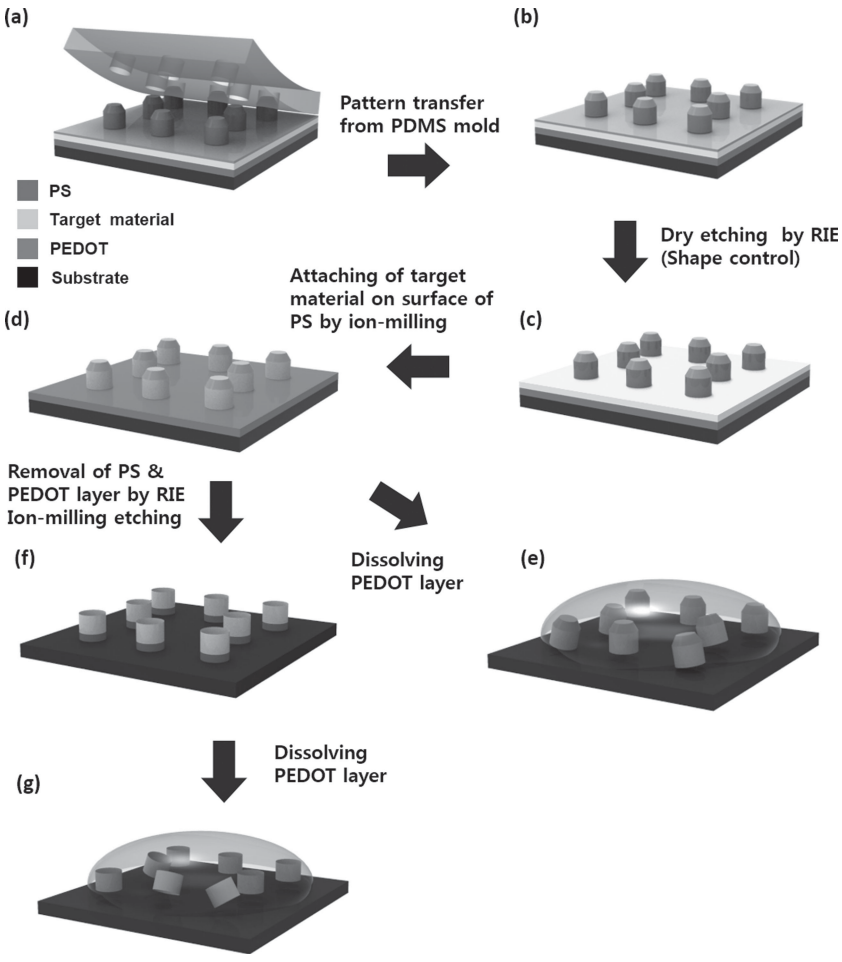

Figure 1. Schematic illustration showing the fabrication of the 3D complex nanoparticles via the top-down SSL method. a) The target material was deposited onto the PEDOT-coated silicon substrate. PS was then spin-coated onto the substrate. b) The PS pillar pattern was transferred by contact with the PDMS mold. c) The PS layer remaining on the bottom was removed by reactive ion etching (RIE). d) The target materials were attached onto the side surfaces of the PS pillar during etching of the target material by Ar ion milling. e) PS-core/Au-shell hybrid SSL nanoparticles were obtained by dissolving the substrate in DI water. f) The PS and PEDOT layers were etched by RIE, and the residual Au layer was removed by ion milling. g) The patterned substrate was immersed in DI water to dissolve the residual PEDOT layer.

2. Results and Discussion

Overall procedures used to fabricate complex monodisperse hybrid nanostructures are illustrated in **Figure 1**. First, a sacrificial PEDOT layer was spin-coated onto an O_2 plasma-treated silicon wafer. The sacrificial layer facilitated the transfer of the prepared nanopatterns onto a silicon wafer by immersion in an aqueous solution. PEDOT was selected as the sacrificial layer because it provided a high thermal stability and good uniformity on the substrate.[35] A target material was deposited on the PEDOT-coated silicon substrate surface by electron beam evaporation. A polystyrene (PS) solution was spin-coated onto the target material, and a pre-patterned PDMS mold was placed on the PS surface to introduce the desired pattern onto the PS surface (Figure 1a). As the PS–PDMS structure was heated above the PS glass transition temperature (T_g), capillary forces drove the polymer into the void spaces of the PDMS mold (Figure 1b).[36] Once the PS pattern had been formed, the PS residue on the surface was removed by reactive ion etching (RIE) using a mixture of O_2 and CF_4 plasma (Figure 1c) to generate a PS pattern on the coated substrate surface. The sizes and shapes of the PS pattern could be controlled by isotropic or anisotropic etching during the etching process.[24] Chair-shaped nanoparticles were formed by tilting the patterned PS substrate during etching by an angle of 35 degrees. Ion milling of the pre-patterned surface using Ar gas was then used to attach the target material to the side walls of the PS pattern through ion bombardment.[32] A variety of nanopattern shapes could be obtained, depending on the PS pattern (Figure 1d). Any target material may be sputtered onto the patterned substrate using accelerated Ar ions. The outcome of the sputtering process will

depend on the power of the accelerated Ar ions, the sputtered target material, and the sputtering angle. At a low power acceleration, most of the sputtered material bounced off of the substrate surface. A low sputtering angle relative to the substrate resulted in the attachment of the target materials to the side walls of the nanopatterned substrate (see the Supporting Information, Figure S1).[37] Inorganic target materials adhered to the organic walls to fabricate organic–inorganic hybrid nanostructures on the substrate. The predeposited target material could be selected to fabricate a variety of hybrid nanoparticles (Pt, Al, Cu, ZnO).[32] The resulting patterns were detached from the substrate by immersing the sample in a 20 mL vial containing 1.5 mL DI water, which dissolved the sacrificial PEDOT layer under mild sonication. The organic–inorganic hybrid nanoparticles maintained their shapes during the detachment process (Figure 1e). Different nanoparticle shapes could be obtained by introducing additional etching steps. The residual PS layer and target material were removed by RIE etching and ion-milling processes, respectively (Figure 1f). Cylinder-shaped nanoparticles were prepared, as shown in Figure 1g. The detached nanoparticles were imaged by drying a droplet of the suspension in a dry oven at 60 °C for 2 h and then imaging by SEM (Supporting Information Figure S2). The SEM images confirmed that the PS patterns successfully yielded a variety of SSL nanoparticle shapes, and the etching procedure could be used to vary the SSL nanoparticle shapes. The pressure of the RIE etching chamber and the etching time could be varied to yield isotropic or anisotropic modifications to the PS nanopattern shapes. The etched PS patterns were monodisperse and homogeneous over a large length scale. Moreover, we prepared different types of SSL hybrid nanoparticles by simply depositing the different target layers onto a substrate, including nickel (Ni), aluminum (Al), silver (Ag), platinum (Pt) and titanium (Ti) (See the supporting information, Figure S3).

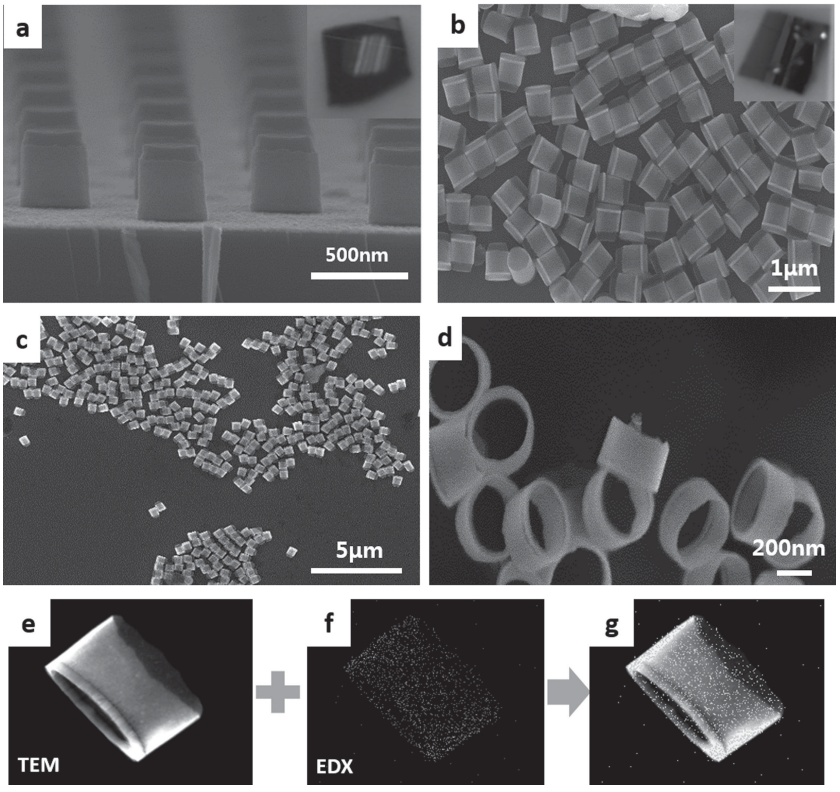

Figure 2. a–c) SEM images of the Au and PS hybrid SSL patterns and the structures of the resulting nanoparticles. a) Au and PS hybrid cylinder nanopattern on a silicon substrate. Inset: optical image of the patterned substrate. b) Detached Au and PS hybrid nanopatterns obtained from the drop and dry process on a silicon bare wafer. Inset: optical image of the wafer after detaching the pattern. c) Large-scale SEM image of the Au and PS nanoparticles obtained from the drop and dry process on a bare silicon wafer. d) Magnified SEM image of SSL ring-shaped Au nanoparticles. e–f) TEM image and 2D EDX mapping image of the SSL ring-shaped Au nanoparticles, and g) combined image.

2.1. Hybrid Core-Shell Nanoparticle Fabrication

Figures 2a and b show SEM and optical images of two representative PS-core/Au-shell hybrid nanopatterns either on a silicon substrate or detached from the substrate, respectively. PS pillars were initially fabricated from a PDMS stamp with a cylinder-shaped master (diameter (d) = 500 nm, spacing (s) = 500 nm, height (h) = 550 nm). After the RIE etching process, the average diameter of the PS pillars was reduced to 300 nm under anisotropic etching.[32] The sizes and shapes of the PS pillars formed from a single master could be varied simply by controlling the PS concentration and etching conditions. The hybrid patterns were highly periodic over large areas, and the patterned regions on the substrate showed a variety of colors, indicating that the patterned structures obeyed Bragg's law (see the inset of Figure 2a). The hybrid nanopatterns were successfully removed from the substrate surface simply by dipping the substrate into an aqueous solution (Figure 2b and 2c). The optical image in the inset of Figure 2b shows the successful detachment of the hybrid nanoparticles after dissolution of the PEDOT sacrificial layer in an aqueous solution. The large-area SEM image (Figure 2c) displays the detached hybrid core–shell nanoparticles. It is important to note that most top-down nanoparticle fabrication methods described previously are carried out in organic solvents and require a solvent exchange procedure.[8] By contrast, our method enables the transfer of nanoparticles directly into an aqueous solution. Thus, our approach is very efficient and provides monodisperse high-quality single and hybrid nanoparticles.

SEM imaging further confirmed that the cylindrical nanoparticles did not suffer from significant distortions (Figure 2d). The lack of distortions could be attributed to the excellent adhesion between the pattern and the substrate surface due to the sputtering characteristics. For example, the sputtered target material adhered strongly to the nanoparticles, which preserved

their shapes during the sputtering and transfer processes. Energy dispersive X-ray (EDX) analysis was carried out to verify that the nanoparticles were generated without considerable contamination. A TEM image (Figure 2e) and the corresponding EDX mapping image (Figure 2f) of a set of cylinder-shaped nanoparticles matched perfectly (Figure 2g), confirming the preparation of highly stable homogenous 3D nanoparticles.

2.2. Monodispersity of SSL Nanoparticle

Until now, top-down fabrication methods are considered as a limited method for mass production. To solve this limitation, accumulation process for nanoparticle concentration increasement is very important in top-down nanoparticle fabrication method. Because most of accumulation process involve centrifugal process, nanoparticle require hardness to endure the centrifugal process in high rpm level. After the concentration increasement process, the size and shape distributions of the nanostructures were next examined (**Figure 3**). Note that most top-down synthesis approaches yield low nanoparticle concentrations, which poses a significant problem in scaling up the synthesis for mass production. Here, the nanoparticle concentration was first increased using a centrifugal separator by aliquotting out five identical cylinder-shaped nanoparticle dispersion samples into centrifugal tube and then centrifuging the samples for 30 min at 15 000 rpm. Including SEM images of the centrifuge-concentrated samples and the original samples indicated that the nanoparticle concentration had increased during centrifugal separation. The SEM results show that the centrifuged samples were four times more concentrated than the original samples (Figure 3a, Supporting S4). The nanoparticle size and shape distributions were characterized by measuring the average heights of the cylinder-shaped nanoparticles (Figure 3b). The nanoparticles were very uniform in shape, and their sizes were narrowly distributed, 270 ± 13 nm. A size distribution histogram was built up by measuring the sizes of several hundred particles taken from 5 different samples.

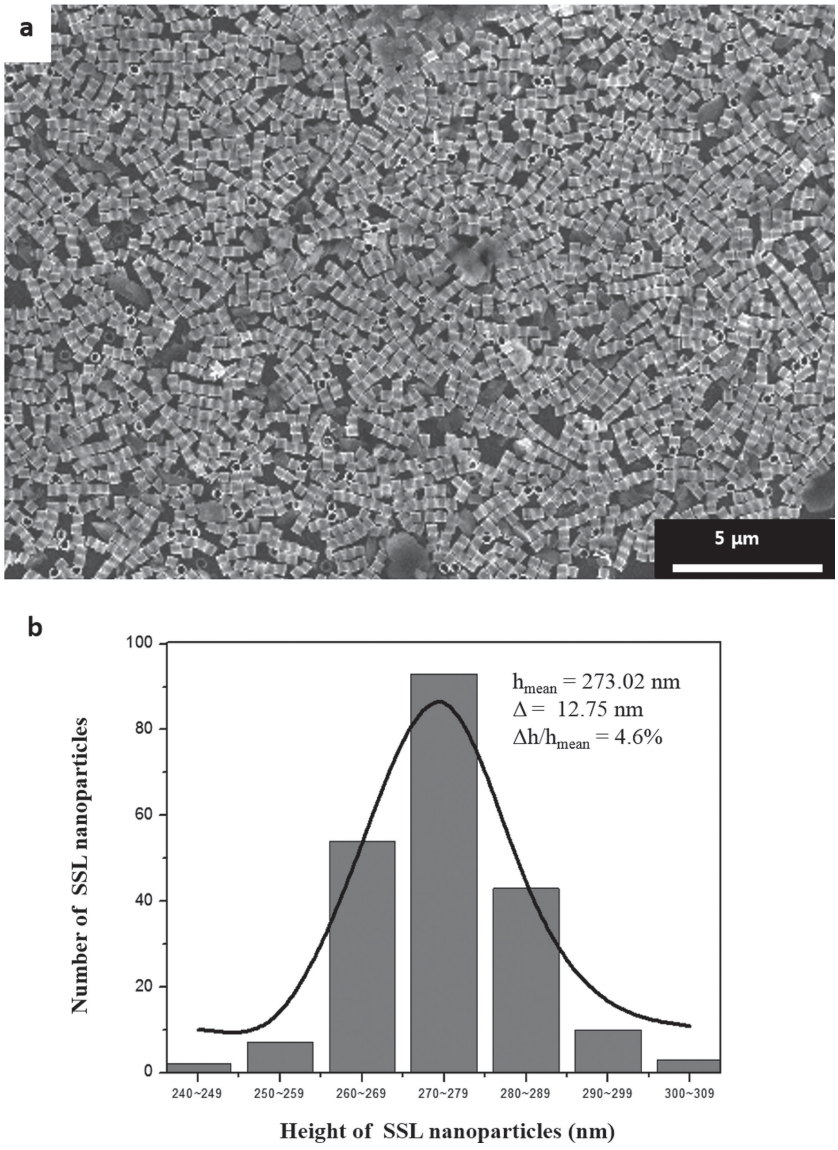

Figure 3. a) Large scale SEM image of SSL nanoparticles after concentraiting in a centrifugal separator. The concentrated solution was dried on a bare silicon wafer. Five samples were fabricated under the same conditions and then concentrated. b) Histogram showing the SSL nanoparticle size distribution. The solid line represents the spline curve of histogram (Scale: nm).

2.3. Verification of SSL Nanoparticle Shape by Etching Condition

This method could be used to generate a variety of complex 3D nanoparticle shapes simply by varying the PS pillar shapes. The shape of the SSL nanoparticles is not only controlled by master but etching condition as well. As a same master, RIE was then applied to create a variety of nanoparticle shapes from a single cylinder-shaped PDMS prepattern. During RIE etching process, plasma etching types are adjustable by vacuum level of reaction chamber (isotropic, anisotropic).[34] Glasses (**Figure 4**a), bowls (Figure 4b), and chairs (Figure 4c) shaped hybrid nanoparticles could be prepared by changing the etching condition. Especially, glasses shaped SSL nanoparticle (Figure 4a) is obtained by using Ion flux diversion effect.[38] In high aspect ratio structure, electrons generated from plasma in RIE are accumulated at upper part of patterned PS pillar and changed as a negatively charged region, relatively, bottom part of PS pillar is changed as positively charged region. This regional charge difference generates ion flux diversion effect and bend a direction of ion. Bended ions are etched the lower part of PS pillar than the

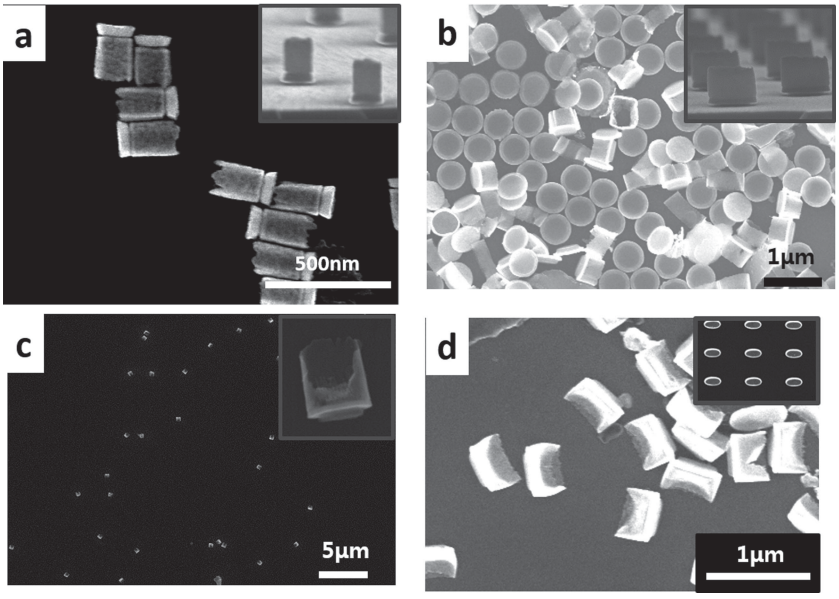

Figure 4. Various shaped nanoparticle fabricated using SSL method. (a–c) Cylinder, glass and bowl shaped SSL nanoparticle fabricated by modifying sequences of etching process. These SSL nanoparticles were fabricated from same master mold. (d) Ellipse shaped SSL nanoparticle fabricated from ellipse shaped master mold.

upper part of PS pillar, thus, a glasses shaped SSL nanoparticle (Figure 4a). Depending on the shape of the pre-patterned substrate (Figure 4d), ellipse shaped SSL nanoparticles are also obtained.

2.4. Size Control of SSL Nanoparticle by RIE Time and PS Concentration

We found that the size of SSL nanoparticle could be controlled by changing the etching time and PS concentration. Initial height of SSL nanoparticle was primarily determined by PS concentration due to capillary phenomena,[34] and further size control (diameter and height) of the Au and PS hybrid SSL nanoparticles was carried out by changing the etching time. Similar heights were observed at a PS concentration (3 wt%), but the diameter of the cylinders was much reduced as etching time increase (**Figure 5**a–c). However, height of SSL nanoparticle was significantly reduced at a lower PS condition (1 wt%) (Figure 5d–g). This is the consequence of the fact that sidewall of PS pillar is etched more than the upper part of one at the low vacuum condition, because upper part of PS pillar is charged as a negative region and repel the plasma ion during etching process.[38] Thus, control of nanoparticle height is dominant to the PS concentration than RIE time.

2.5. Encapsulation of Fluorescent Dye in Core-Shell Hybrid Nanoparticles

In an effort to demonstrate the utility of the core–shell hybrid nanoparticles for biosensing applications, a fluorescent dye, fluorescein isothiocyanate (FITC), was introduced into the organic core of the nanoparticle. FITC was encapsulated into the hybrid nanoparticles by mixing a 0.1 wt% FITC solution into the 4 wt% PS solution in a 1: 1 ratio during the substrate preparation process. The FITC/PS solution was spin-coated onto a prepared substrate, and the structure was then used to fabricate polymer pillars (see Figure 1a). Confocal microscopy imaging confirmed that the fluorescence signal of the SSL nanoparticles could be detected (**Figure 6**a,b). Although the SSL nanoparticles could be detached from the substrate and transferred to a glass substrate, confocal signals were only observed from the SSL nanoparticle clusters (Figure 6c,d). The FITC-encapsulated hybrid nanoparticles are particularly suitable for bioimaging applications because the plasmon resonance of the thin Au layer structure in the hybrid nanoparticles yielded an enhanced fluorescence yield. The enhanced fluorescence

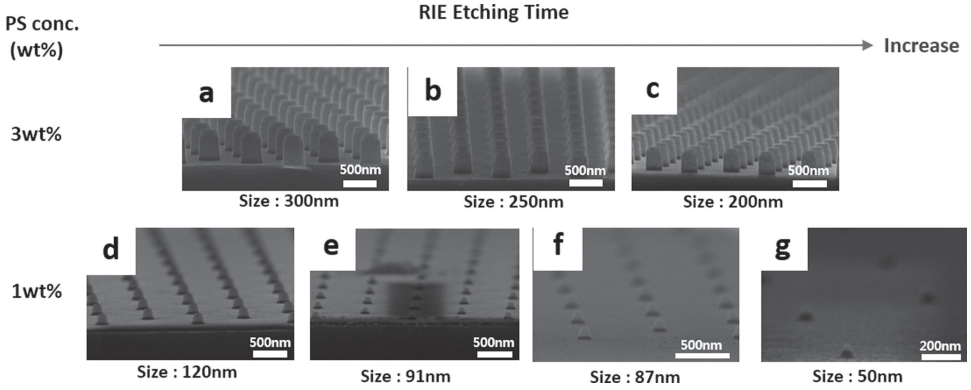

Figure 5. Various sizes of SSL hybrid Au nanoparticle by controlling RIE time and PS concentration. SSL hybrid nanoparticles in the range of 300 nm to 50 nm were fabricated from a single PDMS mold (diameter (d) = 500 nm, center to center spacing = 1000 nm, height (h) = 450 nm): (a) d: 300 nm, h: 398 nm, RIE time: 60 s. (b) d: 250 nm, h: 385 nm, RIE time: 90 s. (c) d: 200 nm, h: 370 nm, RIE time: 120 s. (d) d: 120 nm, h: 120 nm, RIE time: 170 s (e) d: 91 nm, h: 71 nm, RIE time: 190 s. (f) d: 87 nm, h: 101 nm, RIE time : 200 s. (g) d: 50 nm, h: 48 nm, RIE time: 240 s.

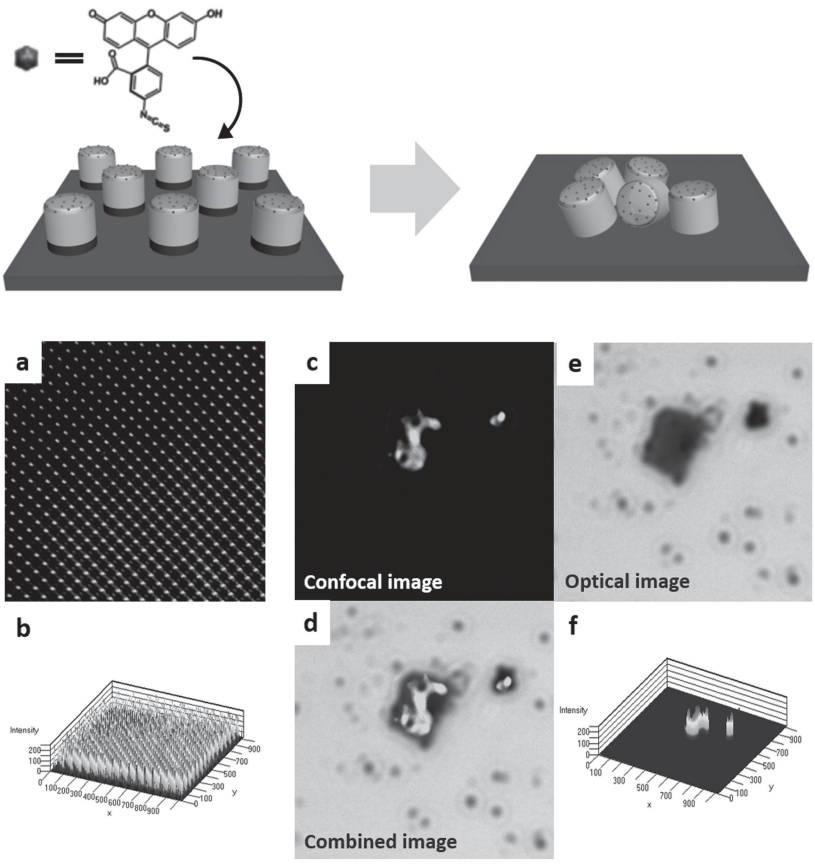

Figure 6. a) Confocal image of the fluorescent organic dye-encapsulating hybrid nanopatterns, and b) two-dimensional fluorescence intensity data prior to the detachment procedure. c) Confocal image, e) optical image, and d) combined image of the fluorescent organic dye-encapsulating hybrid nanoparticles after detachment from the glass substrate. f) Two-dimensional fluorescence intensity data after nanoparticle detachment.

intensity of the hybrid nanoparticle was modeled using FDTD simulations, the results of which agreed well with the experimental results.[39]

3. Conclusions

We developed a method for fabricating monodisperse single-component or core–shell hybrid nanoparticles via a unique top-down SSL approach. The shapes of the fabricated nanoparticles could be controlled by changing the etching conditions and etching sequence to generate a variety of complex nanoparticles that are difficult to prepare using conventional fabrication methods. Not only the shape of nanoparticle, but also the size of one was controlled from 500 nm to 50 nm by a single master mold. The compositions of the hybrid nanoparticles could be varied and any inorganic target material could be used according to the SSL method, provided that the physical adhesion between the organic and inorganic components was stable. After the nanoparticle fabrication, we successfully detached and accumulated monodisperse nanoparticles without any distortion. Moreover, we confirmed that SSL hybrid nanoparticles can contain the fluorescence dye in core-part and show fluorescence imaging signal as a optical carrier material.

4. Experimental Section

Nanoparticle Fabrication: A silicon wafer was treated with O_2 plasma for 3 min. This treatment increased the adhesion between the PEDOT layer (PH500, AI4083 H.C Starck) and the wafer. A uniform PEDOT layer was formed by spin-coating the PEDOT solution onto the wafer (3000 rpm, 45 s). A syringe filter (DISMIC-13_{CP}, Cellulose Acetate, 0.20 μm) was used to filter out PEDOT aggregates. A Cr:target material (thickness = 4:40 nm) bilayer was deposited by e-beam evaporation onto the PEDOT-coated silicon wafer. Onto the prepared substrate was spin-coated a thin film of polystyrene (molecular weight 20 kg mol^{-1}) to form a polymer resist. The cured PDMS (Sylgard 184, Dow Corning; 10:1 ratio of prepolymer to curing agent) mold with topographic features was placed onto the polymer film to fabricate PS patterns upon heating at 135 °C for 2 h. The resulting PS pillar array on the substrate was subsequently removed under O_2/CF_4 RIE (40/60 sccm, pressure (20 mTorr), RF power (80 W)). An ion-milling process was applied to the pre-patterned surface using Ar^+ gas. The target material attached to the side walls of the PS pattern through ion bombardment, and various hybrid nanoparticle shapes could be obtained, depending on the shapes of the PS pillars. The nanoparticle array was then immersed in 1 mL DI water to remove the PEDOT layer. The organic/inorganic hybrid nanoparticles maintained their shapes during the detachment process.

Encapsulation of a Fluorescent Dye in the Hybrid Nanoparticles: Fluorescein isothiocyanate (FITC, available from Aldrich) was dissolved in an ethanol solution to 0.1 wt%. The FITC solution was mixed with a 4 wt% polystyrene (Aldrich) solution in a 1:1 ratio and then shaken for 5 min. The solution was spin-coated onto a prepared substrate (Au/PEDOT/Silicon) and patterned using a PDMS mold. The procedures described above for the fabrication of hybrid nanoparticles were then applied to the sample.

Characterization: FE-SEM with EDS (Sirion) and FE-TEM (Tecnai G^2 F30 S-Twin) were used to collect nanoparticle images and to confirm the material composition. Fluorescence images were collected by confocal microscopy (Carl Zeiss, LSM510 META NLO) using a 488 nm argon laser (with a 568 nm low-pass filter).

Supporting Information

Supporting Information is available from the Wiley Online Library dor from the author.

Acknowledgements

This research was supported by the WCU (World Class University) program (R32–2008–000–10142–0) through the National Research Foundation of Korea, the center for advanced Soft Electronics under the Global Frontier Research Program(No, 2011–0032062) funded by the Ministry of Education, Science and Technology, Korea. And this research

was supported by the National Research Foundation of Korea(NRF) grant funded by the Korea government(MEST) (No. 2012R1A2A1A01003537). SEM experiments were carried out at NNFC in KAIST.

Received: July 25, 2013
Published online: August 27, 2013

[1] B. D. Chithrani, A. A. Ghazani, W. C. Chan, *Nano Lett.* **2006**, *6*, 662.
[2] E.-K. Lim, Y.-H. Huh, J. Yang, K. Lee, J.-S. Suh, S. Haam, *Adv. Mater.* **2011**, *23*, 2436.
[3] N. G. Portney, K. Singh, S. Chaudhary, G. Destito, A. Schneemann, M. Manchester, M. Ozkan, *Langmuir* **2005**, *21*, 2098.
[4] J. Y. Chen, B. Lim, E. P. Lee, Y. N. Xia, *Nano Today* **2009**, *4*, 81.
[5] S.-W. Lee, S. K. Lee, A. M. Belcher, *Adv. Mater.* **2003**, *15*, 689.
[6] H. S. Choi, Y. Ashitate, J. H. Lee, S. H. Kim, A. Matsui, N. Insin, M. G. Bawendi, M. Semmler-Behnke, J. V. Frangioni, A. Tsuda, *Nat. Biotechnol.* **2010**, *28*, 1300.
[7] X. Hu, J. Gong, L. Zhang, J. C. Yu, *Adv. Mater.* **2008**, *20*, 4845.
[8] W. Hu, M. Zhang, R. J. Wilson, A. Koh, J.-S. Wi, M. Tang, R. Sinclair, S. X. Wang, *Nanotechnology* **2011**, *22*. 185302.
[9] Y. Yao, L. Hu, N. Liu, M. T. McDowell, W. D. Nix, I. Ryu, Y. Cui, *Nano Lett.* **2011**, *11*, 2949.
[10] Z. Peng, H. Yang, *Nano Today* **2009**, *4*, 143.
[11] Y. Y. Ma, W. Y. Li, E. C. Cho, Z. Y. Li, T. K. Yu, J. Zeng, Z. X. Xie, Y. N. Xia, *ACS Nano* **2010**, *4*, 6725.
[12] M. Li, K. T. A. Jamal, K. Kostarelos, J. Reineke, *ACS Nano* **2010**, *4*, 6303.
[13] Y. Xia, Y. Xiong, B. Lim, S. E. Skrabalak, *Angew. Chem. Int. Ed.* **2009**, *48*, 60.
[14] D. M. Jeffrey, A. Gerbec, A. Washington, G. F. Strouse, *J. Am. Chem. Soc.* **2005**, *127*, 15791.
[15] S. H. Ahn, L. J. Guo, *Adv. Mater.* **2008**, *20*, 2044.
[16] S. J. Jeong, H.-S. Moon, J. Shin, B. H. Kim, D. O. Shin, J. Y. Kim, Y.-H. Lee, J. U. Kim, S. O. Kim, *Nano Lett.* **2010**, *10*, 3500.
[17] J. S. Park, S. H. Lee, T. H. Han, S. O. Kim, *Adv. Funct. Mater.* **2007**, *17*, 2315.
[18] J. Y. Kim, B. H. Kim, J. O. Hwang, S.-J. Jeong, D. O. Shin, J. H. Mun, Y. J. Choi, H. M. Jin, S. O. Kim, *Adv. Mater.* **2013**, *25*, 1331.
[19] J. P. Rolland, B. W. Maynor, L. E. Euliss, A. E. Exner, G. M. Denison, J. M. DeSimone, *J. Am. Chem. Soc.* **2005**, *127*, 10096.
[20] J. Y. Kelly, J. M. DeSimone, *J. Am. Chem. Soc.* **2008**. *130*, 5438.
[21] M. J. Hampton, J. L. Templeton, J. M. DeSimone, *Langmuir* **2010**, *26*, 3012.
[22] T. J. Merkel, K. Chen, S. W. Jones, A. A. Pandya, S. Tian, M. E. Napier, W. E. Zamboni, J. M. DeSimone, *J. Controlled Release* **2012**, *162*, 37.
[23] J.-Y. Wang, Y. Wang, S. S. Sheiko, D. E. Betts, J. M. DeSimone, *J. Am. Chem. Soc.* **2012**, *134*, 5801.
[24] B. Lim, J. Jang, *Angew. Chem. Int. Ed.* **2003**, *42*, 5600.
[25] J. F. R. H. Liu, J. F. Rusling, N. Hu, *Langmuir* **2004**, *20*, 10700.
[26] A. Nan, R. Turcu, J. Liebscher, *J. Polym. Sci. Part A: Polym. Chem.* **2011**, *50*, 1485.
[27] S. Gai, P. Yang, C. Li, W. Wang, Y. Dai, N. Niu, J. Lin, *Adv. Funct. Mater.* **2010**, *20*, 1166.
[28] M. M. Shahjamali, M. Bosman, S. Gao, X. Huang, S. Seedat, E. Martinsson, D. Aili, Y. Y. Tay, B. Liedberg, S. C. J. Loo, H. Zhang, F. Boey, C. Xue, *Adv. Funct. Mater.* **2012**, *22*, 849.
[29] J. Zhang, M. Post, T. Veres, Z. J. Jakubek, J. Guan, D. Wang, F. Normandin, Y. Deslandes, B. Simard, *J. Phys. Chem. B.* **2006**, *110*, 7122.
[30] Y. T. Lim, O. O. Park, H.-T. Jung, *J. Colloid Interf. Sci.* **2003**, *263*, 449.
[31] D. Aherne, D. E. Charles, M. E. Brennan-Fournet, J. M. Kelly, Y. K. Gun'ko, *Langmuir* **2009**, *25*, 10165.
[32] H.-J. Jeon, K. H. Kim, Y.-K. Baek, D. W. Kim, H.-T. Jung, *Nano Lett.* **2010**, *10*, 3604.
[33] H. S. Jeong, H.-J. Jeon, Y. H. Kim, M. B. Oh, P. Kumar, S.-W. Kang, H.-T. Jung, *NPG Asia Mater.* **2012**, *4*, e7.
[34] H.-J. Jeon, H.-W. Yoo, E. H. Lee, S. W. Jang, J.-S. Kim, J. K. Choi, H.-T. Jung, *Nanoscale* **2013**, *5*, 2358.
[35] W. H. Kim, G. P. Kushto, H. Kim, Z. H. Kafafi, *J. Polym. Sci. Part B: Polym. Phys.* **2003**, *41*, 2522.
[36] J.-M. Jung, F. Stellacci, H.-T. Jung, *Adv. Mater.* **2007**, *19*, 4392.
[37] J. J. Cuomo, H. R. Kaufman, *Handbook of Ion Beam Processing Technology: Principle, Deposition, Film Modification and Synthesis*, Noyes Publ, Park Ridge, NJ **1989**, p.438.
[38] K. Y. Yeom, Plasma Etching Technology, Young, Seoul 2006, p.208.
[39] H.-J. Jeon, H.-W. Yoo, J.-S. Kim, H.-T. Jung, unpublished.